1. SLIDING MODE CONTROL

Sliding mode control [Utkin] is a form of bang-bang control in which the plant state is forced towards and maintained within a close vicinity of a boundary determined by the control system designer.

1.1. Variable Structure Concept and Phase Portrait

A variable structure system is defined as a dynamical system, which changes structure as a function of its state and external input variables.

The most often systems have two structures only, (S_1) and (S_2), between which it switches according to a switching function $S(\mathbf{x},y_r)$. For illustration as example consider the variable structure system of Fig. 1. The system consists of two integrators connected in cascade. According to switch position if negative feedback is closed then system forms structure, (S_1) and if positive feedback is closed system forms structure (S_2).

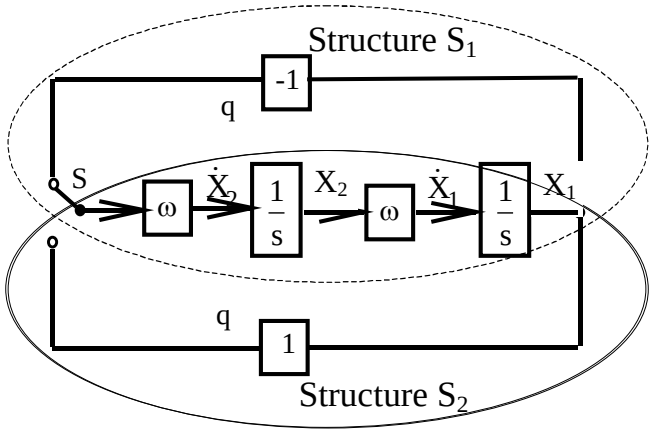

Fig. 1. Variable structure system for study of phase portrait

The state differential equations may be seen direct from block diagram of Fig. 1 as follows:

$$\dot{x}_1 = \omega x_2$$
$$\dot{x}_2 = q\omega x_1 \qquad (1a,b)$$

where q=-1 for structure S_1 and q=1 for structure S_2. If the second equation is divided with the first one, the separable differential equation has form:-

$$\frac{dx_2}{dx_1} = \frac{qx_1}{x_2} \qquad (2)$$

This is first order differential equation which has for non-zero initial states solution:-

$$x_2^2 - qx_1^2 = x_2^2(0) - qx_1^2(0) \qquad (3)$$

For structure S_1 with q=-1 it represents a family of circles centred around origin and for structure S_2 with q=1 it represents a family of hyperbolas symmetrical about the origin as it is shown in Fig. 2.

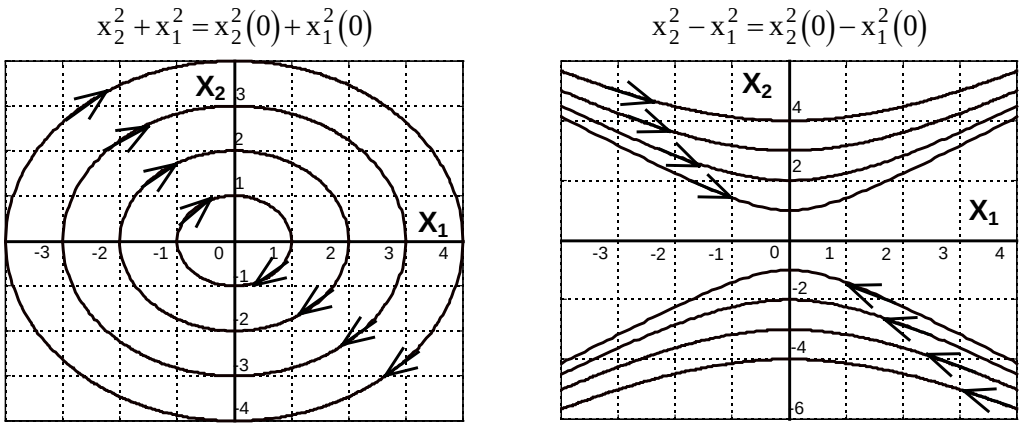

Fig. 2. Phase portraits for variable structure separately

It is important to determine the direction of motion along the state trajectories. This can be done by examination of the state differential equations. Equation (1a) indicates that x_1 must be increasing for $x_2>0$ and similar way equation (1b) indicates that x_1 must be decreasing for $x_2<0$.

Next step is to determine closed-loop phase portrait. For this purpose it is necessary to determine switching function for the switch S. In this special theoretical case two switching boundaries are determined as:-

$$x_1 = 0$$
$$x_2 = -kx_1 \qquad (4)$$

In this case the state trajectories for the complete variable structure system can be drawn for any initial state. The switching always occurs when trajectories cross the switching boundaries defined as (4). Closed-loop phase portrait of variable structure system is shown in Fig. 3.

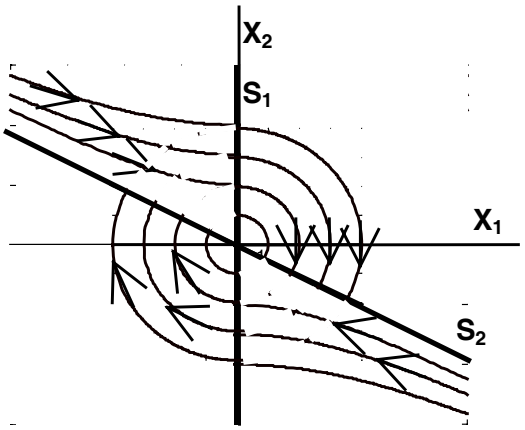

Fig. 3. Closed-loop phase portrait of variable structure system

1.2. Sliding Motion and Mode Control

Now it is possible to create control system, which has variable structure. If the original switch S is replaced with signum function and switching between two values of voltage U_m is now determined by the control system designer then a practicable sliding mode controller shown in Fig. 4 is design:-

$$u = U_m \text{sign}(S) \tag{5}$$

where S is switching function. Let for the second order control system is switching function S determined as:-

$$S = \omega_d - \omega_r - T_\omega \dot{\omega}_r \tag{6}$$

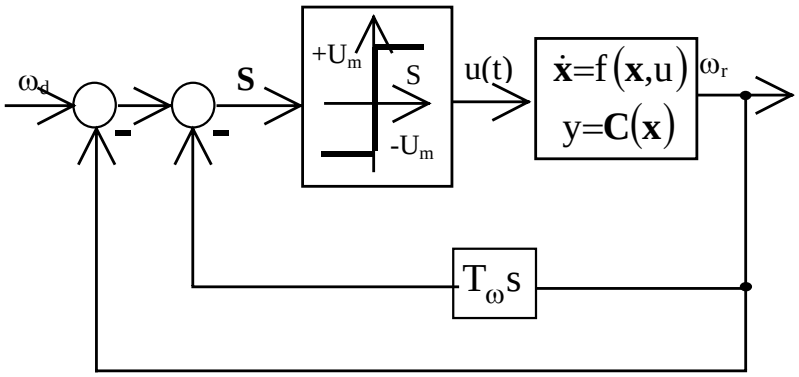

Fig. 4. A practicable sliding mode controller for SISO plant

The operation of such a control loop may be examined in the phase-plane, i.e, the graph of $\dot{\hat{\omega}}_r$ against $\hat{\omega}_r$. The control, u(t), switches between $+U_m$ and $-U_m$, when $S = 0$. Setting this condition in (6) then yields the *switching boundary*. This is shown in Fig. 5 together with a family of state trajectories commencing from different starting points (referred to as a *phase portrait*).

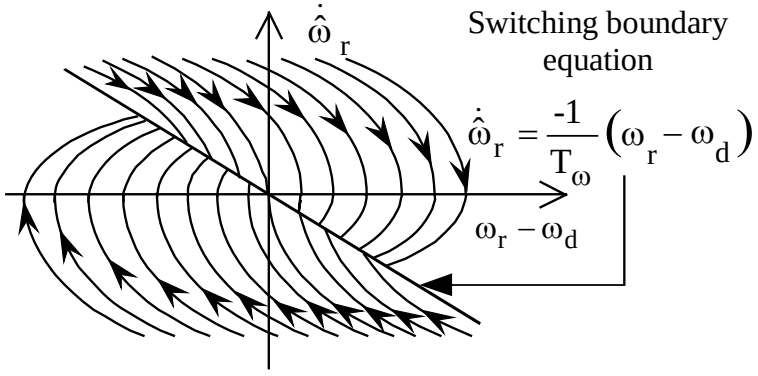

Fig. 5. Closed-loop phase portrait and switching boundary for sliding mode control of SISO system

It is evident that over most of the boundary shown, the *trajectories of the phase portrait are directed towards the boundary from both sides*, meaning that once the boundary is reached, the trajectory is maintained close to it while the control variable, u(t), rapidly switches (*control chatter*). This is the condition for sliding motion and the controller described is the classical sliding mode controller. Under these circumstances, the closed-loop system obeys the switching boundary equation (7) shown in Fig. 5.

$$\frac{\omega_r(s)}{\omega_d(s)} = \frac{1}{1+sT_\omega} \tag{7}$$

The ideal sliding mode control system will have a control variable with an infinite switching frequency and continuously varying mark space ratio, holding the phase plane trajectory precisely on the switching boundary during the sliding mode. In this case, the continuous short term mean control variable, obtainable by filtering out only the finite frequency components of u(t), would also hold the sub-state trajectory y(t), precisely on the switching boundary. In this sense, the '*continuous short term mean'* of control variable is equivalent to the ideal switch control. For this reason the short term mean control variable is referred to as the equivalent control.

In the real system the variable structure exhibits sliding motion along the segments of a switching boundary towards which the state trajectories of the closed loop phase portrait are directed from both sides. This is clearly evident from the sliding mode of phase trajectory shown in Fig. 6.

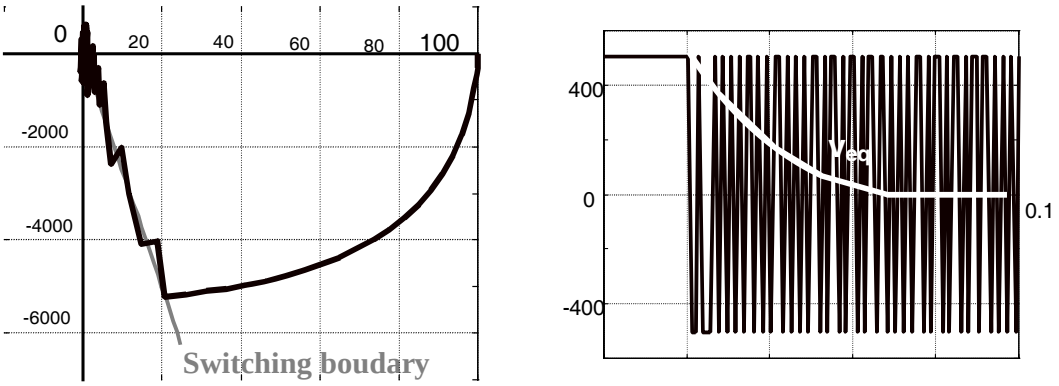

Fig. 6. Sliding motion of the real variable structure system

In its basic form as t is shown in Fig. 4, sliding mode control is a form of bang-bang state feedback control in which the control variable, u(t), switches between two limits of the opposite signs. Bang-bang control systems are sometimes referred to as 'relay' or 'on-off' systems [Jemeljanov, Utkin].

If, for a SISO plant, the state variables are chosen as the controlled output and its derivatives up to an order equal to '*R-1'*, where '*R*' is the plant rank, then if the state is maintained precisely on the boundary, the closed loop dynamics is determined by the boundary alone and is *independent of the plant parameters and any external disturbances.* As it can be seen from Fig. 6, *t*he state point then appears to *slide* in the boundary. Hence the term *sliding motion* is used. Since the boundary is an '*R-1'*

dimensional hyper-surface in an '*R*' dimensional output derivative space, the order of the closed-loop system in the sliding mode is always '*R-1*'. This fact is made use of in the general sliding mode controller for SISO linear plant:-

$$S\left(y_r, y, \dot{y}, \ddot{y}, ..., y^{R-1}\right) = y_r - \left(y + q_1\dot{y} + q_2\ddot{y} + ... + q_{R\text{-}1}y^{R-1}\right) \tag{8}$$

Corresponding control structure is shown in Fig. 7. More general formula for switching function is as follows:-

$$S(\mathbf{y}, y_r) = y - y_r - \sum_{i=1}^{R-1} q_i y^{(i)} \tag{9}$$

where $y = \left[y\ \dot{y}\ ...\ y^{(R-1)}\right]^T$ is a vector of state variables comprising the controlled output and its derivatives and R is the rank of the plant (i.e. *the number of poles minus number of zeros of the transfer function in the case of a linear plant*). Whenever the switching function S changes its sign what corresponds to equation:-

$$S(\mathbf{y}, y_r) = 0 \tag{10}$$

all the values of **y** at which switching of u(t) takes place are determined what is referred as a boundary equation.

Fig. 7 shows general sliding mode control system for SISO linear plant.

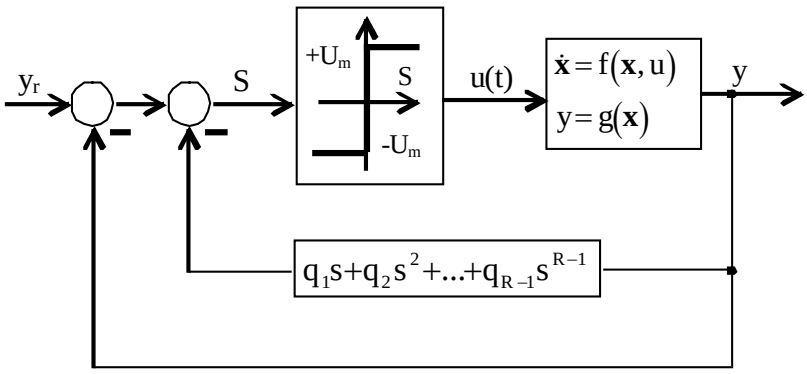

Fig. 7 General sliding mode control system for SISO linear plant

In the ideal system where the switching in the sliding mode is at an infinite frequency, equation (6) governs the closed-loop behavior and since $x_1 = y$ and $x_2 = \dot{y}$, the closed loop system is linear with a first order transfer function (7), The important observations to be made here are:

a) The system is extremely robust since transfer function (7) is independent of the plant parameter and the load torque (referred to the control voltage), u(t).
b) The closed-loop system is only of first order despite the plant being of second order. This is due to one degree of freedom of movement in the state space being removed by the control law forcing the trajectory to move along the switching boundary.
c) The settling time, T_s, may be chosen and the closed-loop time constant is $T_\omega = T_s/3$.

It is important to realize that the above ideal characteristic (a) cannot be attained precisely in practice due to the finite sampling frequency of the digital implementation and any dynamic lags that are not taken into account (*such as the armature time constant in the d.c. drive example*). The performance of a practicable sliding mode control system must be predicted by an accurate simulation.

1.3. Elimination of Control Chattering

In some applications, the rapid switching of the control variable, referred to as *control chatter*, is undesirable. A common method for eliminating this is to replace the signum function of the control law:-

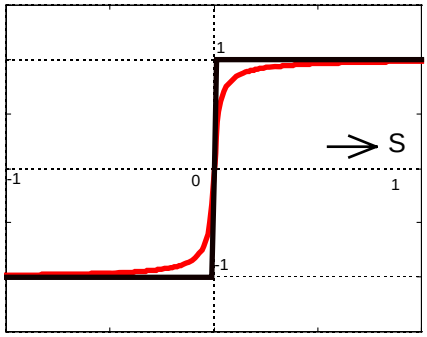

$$u = U_{max} \cdot \text{sign}(S) \qquad (11)$$

$$u = U_{max} \cdot \frac{S}{|S| + \delta}$$

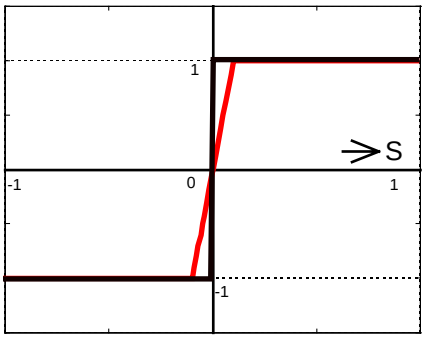

$$u = U_{max} \cdot \text{sign}(S) \qquad (12)$$

$$u = U_{max} \cdot \text{sat}(K, S)$$

Fig. 8a,b. Two common smooth approximations of the signum function

In the case of Ambrosino's approximation, (11), the control *never* reaches the saturation limits but asymptotically approaches them as S increases in magnitude. A sharp transition of the control between extreme values approaching saturation occurs whenever S changes sign.

A similar performance results from using the saturation function (12), see Fig. 8b. In this case, the switching boundary is replaced by a finite control transition region called the *boundary layer*, outside of which the control saturates at $\pm U_m$.

A completely different approach is to insert a **smoothing integrator** between the rapidly switching control variable (*renamed now as u'(t)*) and actual control variable u(t) applied to plant. The control smoothing integrator may be considered as a part of a new plant to be controlled. It means that the rank of the original plant was increased by one unit. Therefore it is necessary to include one more derivative due to order '*R*+1'of a 'new' system as it is shown in Fig. 9.

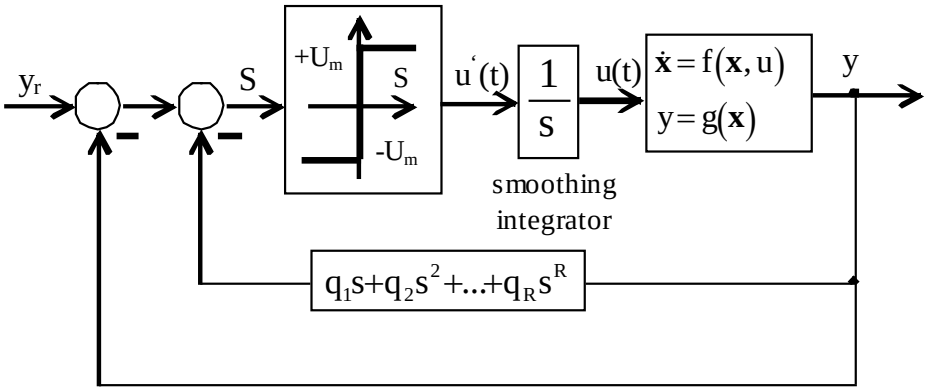

Fig. 9. SMC system with control smoothing integrator

The effect of the smoothing integrator on control variable u(t) can be clearly observed from Fig, 10.

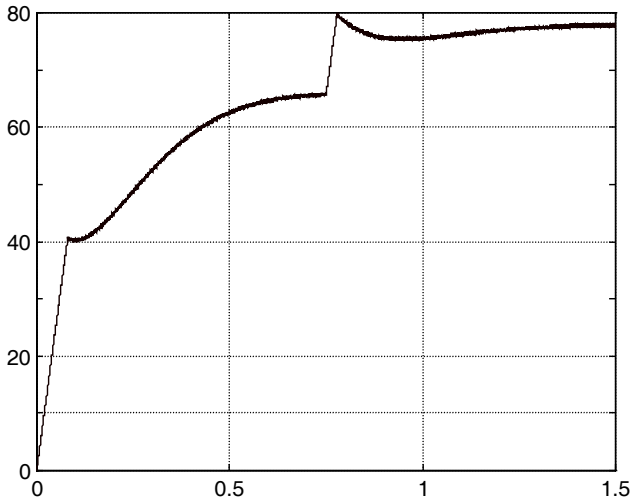

Fig. 10. Control variable u(t) of SMC system with control smoothing integrator

1.4. Sliding Mode Control of an Induction Motor

Consider now the closed-loop system which consists of non-linear control law based on feedback linearisation and induction motor, which has the nominal transfer function (13).

$$\frac{\hat{\omega}_r(s)}{\omega_d(s)} = \frac{1}{1+sT_\omega} \tag{13}$$

Since the IM is inherently nonlinear, errors introduced by uncertainties of its parameter will cause the linear dynamics of (7) to become nonlinear. It may be shown, that the sliding mode outer control loop can compensate for this. To illustrate this

action more simply, let parametric uncertainties, external load torque and imperfect operation of the inner control loop due to the non-zero iteration interval will (*roughly*) be represented by a change of time constant and DC gain. Then the combined inner and middle loop dynamics resulting from the aforementioned errors and disturbances may be represented by the transfer function:-

$$\frac{\hat{\omega}_r(s)}{\omega'_d(s)} = \frac{K_d}{1+sT'_\omega} \tag{14}$$

where $K_d > 0 \,\&\, \neq 1$ and $T'_\omega > 0 \,\&\, \neq T_\omega$. In order to create a sliding mode control loop that does not reduce the system order (equal to the rank without transfer function zeros), which is required to yield the closed-loop system dynamics of (7), a smoothing integrator is introduced at the speed reference input of the middle control loop. It increases its order by one before formation of the sliding mode outer loop. Fig. 11 shows this, treated as a new plant with control variable, u', and with the outer loop controller.

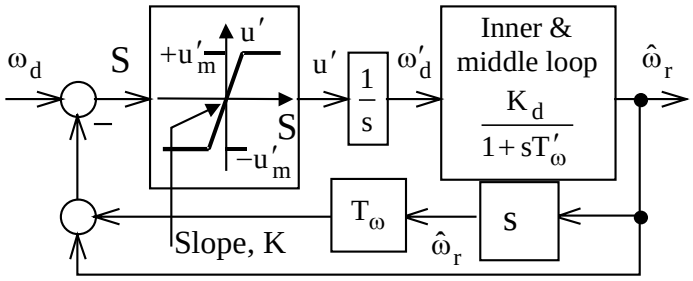

Fig. 11. Sliding mode based outer control loop

Since an angular acceleration as derivation of angular speed would be a subject of substantial noise contamination, an opportunity to use an equivalent outer loop control algorithm avoiding this is taken. With reference to Fig. 12, the integrator effectively cancels the differentiation in the inner feedback loop. The resulting block diagram is shown in Fig. 12 and this yields the SMC based control algorithm of equation (15).

$$\omega'_d = K_{SM}\left\{\int(\omega_d - \hat{\omega}_r)dt - T_\omega\hat{\omega}_r\right\} \tag{15}$$

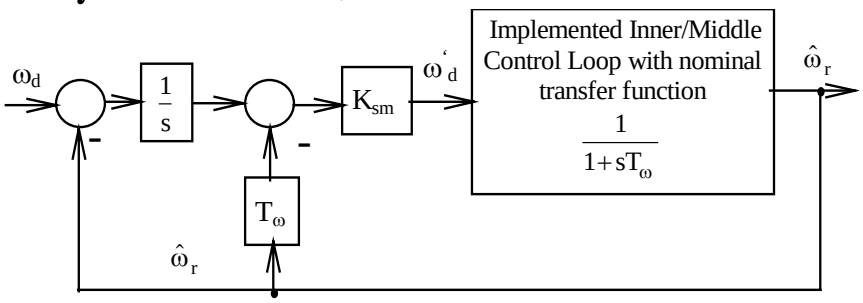

Fig. 12. SMC based outer control loop implemented in experiment with induction motor

The experimental results with this structure are shown in Fig. 13. In all the graphs presented, the stator current and rotor magnetic flux components as functions of time during the starting interval $t \in$(0-0.1) s are shown in subplots (a). The estimates of the

rotor speed from the pseudo-sliding mode observer are shown in subplots (b) as functions of time for the whole data logging interval. Plots (c) show the load torque estimate, $\hat{\Gamma}_L$, from the filtering observer together with the rotor magnetic flux norm estimate $\|\Psi\|$. Finally, subplots (d) show the ideal rotor speed, ω_{id}, together with real rotor speed, ω_r, and its estimate, $\hat{\omega}_r$, from filtering observer for the whole data logging interval. The simulation and experimental results are plotted, respectively, in the left and right columns.

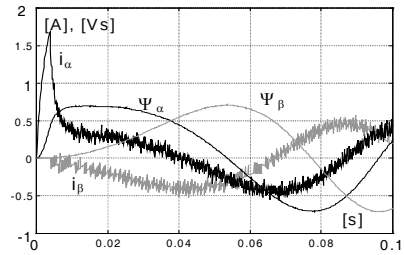

*a1) Stator current and rotor mg. flux components - **simulation***

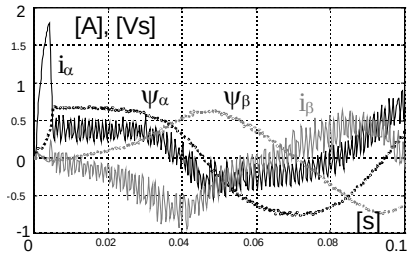

*a2) Stator current and rotor mg. flux components - **experiment***

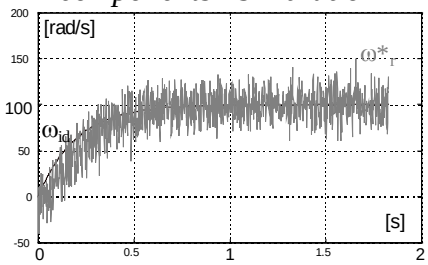

b1) Estimated, unfiltered rotor speed from pseudo-sliding mode observer

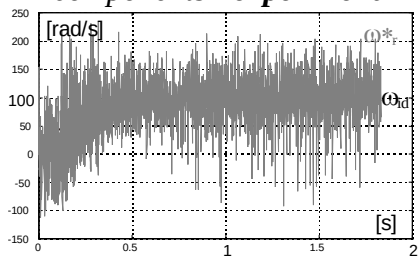

b2) Estimated rotor speed from pseudo-sliding mode observer

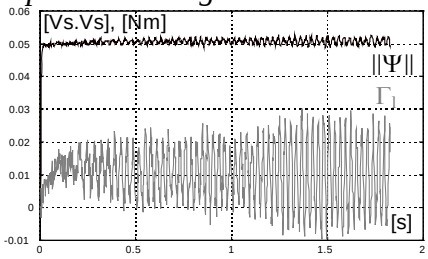

c1) Estimated rotor mg. flux norm and load torque from filtering observer

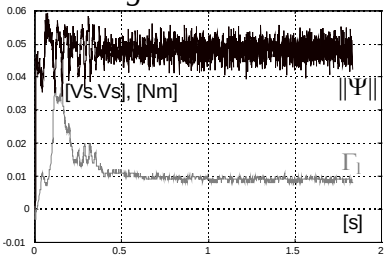

c2) Estimated rotor mg. flux norm and load torque from filtering observer

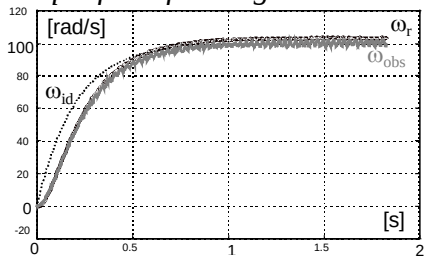

d1) Ideal speed response, real and estimated rotor speed – simulation

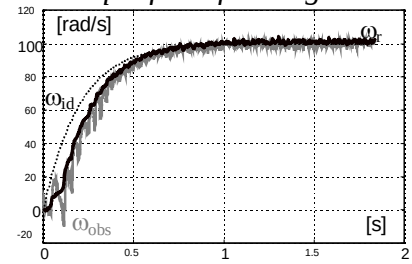

d2) Ideal speed response, real and estim. rotor speed - experiment

Fig. 13. Speed response and corresponding state variables with sliding mode based outer control loop

1.5. Sliding Mode as an Observation Tool

1.5.1. Pseudo-Sliding Mode Observer for Rotor Speed

The following non-linear differential equations formulated in the magnetic field-fixed (*d_q*) co-ordinate system describe the permanent magnet synchronous motor:-

$$\frac{d}{dt}\begin{bmatrix} i_d \\ i_q \end{bmatrix} = \begin{bmatrix} \frac{-R_s}{L_d} & p\omega_r \frac{L_q}{L_d} \\ -p\omega_r \frac{L_d}{L_q} & \frac{-R_s}{L_q} \end{bmatrix} \cdot \begin{bmatrix} i_d \\ i_q \end{bmatrix} - \frac{p\omega_r}{L_q} \begin{bmatrix} 0 \\ \Psi_{PM} \end{bmatrix} + \begin{bmatrix} \frac{1}{L_d} & 0 \\ 0 & \frac{1}{L_q} \end{bmatrix} \cdot \begin{bmatrix} u_d \\ u_q \end{bmatrix} \tag{16a}$$

$$\frac{d\omega_r}{dt} = \frac{1}{J}\left\{c_5\left[\Psi_{PM} i_q + \left(L_d - L_q\right) i_d i_q\right] - \Gamma_L\right\} = \frac{1}{J}\left\{\Gamma_{el} - \Gamma_L\right\} \tag{16b}$$

Magnetic fluxes of the motor are described as:-

$$\begin{aligned} \psi_d^* &= L_d i_d + \Psi_{PM} \\ \psi_q^* &= L_q i_q \end{aligned} \tag{17}$$

The basic '***stator current vector pseudo sliding-mode observer***' is based on equation (16a) as a real time model but *purposely omitting all terms containing ω_r and using only the last term*. Thus:-

$$\frac{d}{dt}\begin{bmatrix} i_d^* \\ i_q^* \end{bmatrix} = \begin{bmatrix} \frac{1}{L_d} & 0 \\ 0 & \frac{1}{L_q} \end{bmatrix} \cdot \begin{bmatrix} u_d \\ u_q \end{bmatrix} + \begin{bmatrix} v_{eq\,d} \\ v_{eq\,q} \end{bmatrix} \tag{18}$$

where $v_{eq\,d}$ and $v_{eq\,q}$ are the model corrections, i^*_d and i^*_q are estimates of i_d and i_q as in a conventional observer. These, however, are not used directly. The useful observer outputs here are the continuous *equivalent values*, (*i.e.*, *the short term mean values*), of the rapidly switching variables **v**;-

$$\mathbf{v} = V_{max} \cdot \mathrm{sgn}(\mathbf{I} - \mathbf{I}^*) \tag{19}$$

Equation (19), of course, cannot directly generate $\mathbf{v_{eq}}$. Instead, a *pseudo-sliding-mode* observer may be formed by replacing equation (19) with:-

$$\begin{bmatrix} v_{eq\,d} \\ v_{eq\,q} \end{bmatrix} = K_{sm} \cdot \begin{bmatrix} i_d - i_d^* \\ i_q - i_q^* \end{bmatrix} \tag{20}$$

where K_{SM} is made as high a gain as possible within the stability limit set by the iteration period of the control algorithm. For large K_{SM} the observer correction inputs closely approximate the terms missing from the real time model, as seen in equation (16a). Thus:-

$$\begin{bmatrix} v_{eqd} \\ v_{eqq} \end{bmatrix} = \begin{bmatrix} \frac{-R_s}{L_d} & p\omega^*_r \frac{L_q}{L_d} \\ -p\omega^*_r \frac{L_d}{L_q} & \frac{-R_s}{L_q} \end{bmatrix} \cdot \begin{bmatrix} i_d \\ i_q \end{bmatrix} - \frac{p\omega^*_r}{L_q} \begin{bmatrix} 0 \\ \Psi_{PM} \end{bmatrix} \tag{21}$$

and an unfiltered angular velocity estimate, ω^*_r, can be extracted from equation (21). The following one of three possible formulae was found to yield the minimum sensitivity to stator current ripple when using the bang-bang algorithm for control of currents:-

$$\omega^*_r = \frac{-\tilde{L}_q v_{eqq} - \tilde{R}_s i_q}{p \cdot \left(\tilde{L}_d i_d + \tilde{\Psi}_{PM}\right)} \tag{22}$$

where the constant motor parameters are replaced by their estimates.

1.5.2. Filtering Observer

If stator current measurement noise is significant, then the system performance will be improved by the provision of filtering. The filtering observer presented produces a filtered angular velocity estimate, $\hat{\omega}_r$ in a similar fashion to a Kalman filter. Finally, there is no direct means of measuring the external load torque, Γ_L. This problem may be easily solved, however, by treating Γ_L as a state variable and including its estimate in the real time model of the observer.

The observer is based on torque differential equation of the motor (16b) and differential equation for load torque, which is assumed constant and so its state equation is $\dot{\Gamma}_L = 0$. Thus, the combined rotor speed and load torque filtering observer is as follows:-

$$\begin{aligned} e_\omega &= \omega^*_r - \hat{\omega}_r \\ \dot{\hat{\omega}}_r &= \frac{1}{\tilde{J}} \left(c_5 \left[\Psi_{PM} i_q + \left(L_d - L_q \right) \cdot i_d i_q \right] - \Gamma_L \right) + k_\omega e_\omega \\ \dot{\hat{\Gamma}}_L &= k_\Gamma e_\omega \end{aligned} \tag{23}$$

This is a second order linear observer with a correction loop characteristic polynomial, which may be chosen via the gains, k_ω and k_Γ, to yield the desired balance of filtering between the noise from the measurements of i_d and i_q and the noise from the angular velocity measurement, ω^*_r. Filtered values of $\hat{\omega}_r$ and $\hat{\Gamma}_L$ can be produced with this linear observer by the adjustment of the one parameter, T_s, only. This is the prescribed steady-state time for observer, which can be determined as:-

$$T_s = 1.5 \cdot (1+n) \frac{1}{\omega_n} \tag{24}$$

With respect of settling time formula (24) for n=2, $\omega_n=9/(2T_s)$, the observer poles can be designed as comparison of left hand side equation wih demanded polynomial and right hand side equation of filtering observer characteristic polynomial:-

$$s^2+\frac{9}{T_s}s+\frac{81}{4T_s^2}=s^2+s\,k_\omega+\frac{k_\Gamma}{J} \tag{25a}$$

$$k_\omega=\frac{9}{T_s}\ \text{ and }\quad k_\Gamma=\frac{81J}{4T_s^2} \tag{25b}$$

A modified version of the observer based on pole placement at two different locations, $-\omega_1$ and $-\omega_2$, which shows higher stability, was used for design of observer gains k_ω and k_Γ. Thus:-

$$s^2+s(\omega_1+\omega_2)+\omega_1\omega_2=s^2+s\,k_\omega+\frac{k_\Gamma}{J} \tag{26a}$$

$$k_\omega=(\omega_1+\omega_2)\ \text{ and }\quad k_\Gamma=J\cdot\omega_1\cdot\omega_2 \tag{26b}$$

Block diagrams of pseudo-sliding mode (*simplified for current torque component, i_q, only*) and filtering observer are shown in Fig. 14a,b.

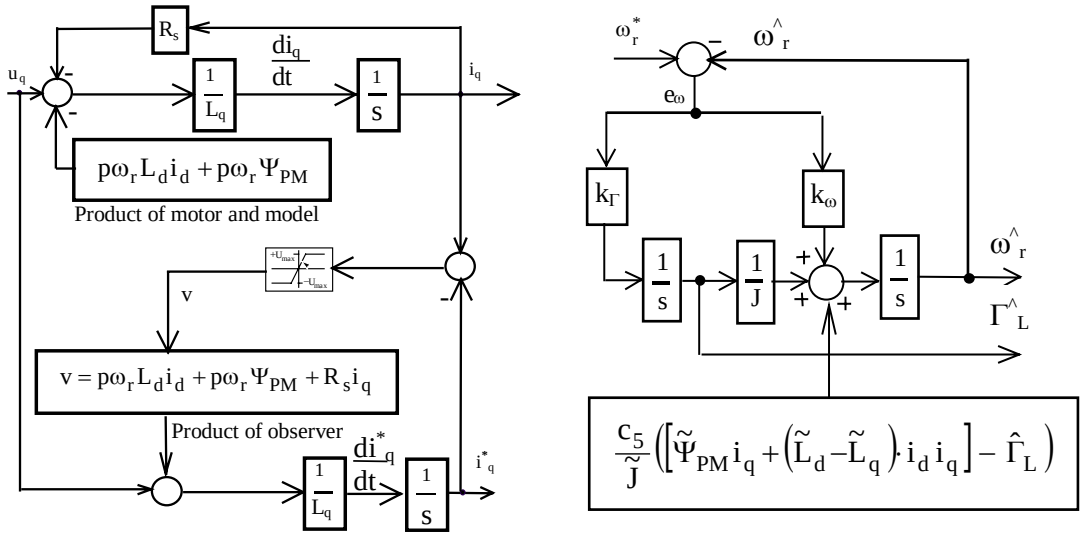

a) Pseudo-sliding mode observer *b) Filtering observer*

Fig. 14. Block diagrams of pseudo-sliding mode and filtering observer